Inorg. Chem. **2008**, *47*, 9518−9527

Inorganic Chemistry
Article

Modeling of the Various Minima on the Potential Energy Surface of Bispidine Copper(II) Complexes: A Further Test for Ligand Field Molecular Mechanics

Alexander Bentz,[†] Peter Comba,*[,†] Robert J. Deeth,*[,‡] Marion Kerscher,[†] Björn Seibold,[†] and Hubert Wadepohl[†]

Universität Heidelberg, Anorganisch-Chemisches Institut, Im Neuenheimer Feld 270, D-69120 Heidelberg, Germany, and University of Warwick, Department of Chemistry, Gibbet Hill Road, Coventry, UK CV4 7AL

Received June 16, 2008

Copper(II) complexes of bispidines (bispidine = tetra-, penta-, or hexadentate ligand, based on the 3,7-diazabicyclo[3.3.1]nonane backbone) display several isomeric forms. Depending on the substitution pattern of the bispidine and the type of coligands used, the structure elongates along one of the three potential Jahn−Teller axes. In an effort to develop a computational tool which can predict which isomer is observed, 23 bispidine−copper(II) complexes with 19 different ligands are analyzed theoretically by ligand field molecular mechanics (LFMM). With two exceptions, the lowest-energy LFMM structure and the experimental solid-state structure agree concerning the Jahn−Teller axis. However, in most cases and especially for six-coordinate complexes, LFMM predicts a second local minimum within a few kilojoules per mole. Although detailed analysis reveals that the current force field is too "stiff", reasonable quantitative reproduction of the structural data is achieved with Cu−L bond length root mean square (rms) deviations for nine complexes of 0.05 Å or less and with 20 reproduced to a rms deviation of 0.1 Å or less. Across all of the complexes, the Cu−amine and Cu−pyridyl bond length rms deviations are 0.07 and 0.12 Å, respectively.

Introduction

Due to the rigidity of the adamantane-derived ligand backbone, the potential energy surface of transition metal bispidine complexes is known to be relatively flat with several shallow minima and steep walls (see Chart 1 for ligand structures). The general and interesting consequence is a high elasticity of the coordination geometry and, more importantly, the possibility to drive the complexes with well-designed modifications of the ligand system, the coligands, or external parameters to one of several close-to-degenerate minimum-energy structures.[1−5] This is important because isomers of this kind are known to have strikingly different properties, such as complex stabilities, redox potentials, electronic structures, and reactivities.[4,6−9]

Of particular interest are copper(II) complexes, which may, due to the inherent Jahn−Teller instability of the d^9 electronic configuration in O_h symmetry, display three tetragonally elongated minimum structures. These structures, the corresponding, usually less stable, compressed geometries and the intervening rhombic structures derived

* Authors to whom correspondence should be addressed. Fax: +49-6221-548453. E-mail: peter.comba@aci.uni.heidelberg.de (P.C.); r.j.deeth@warwick.ac.uk (R.J.D.).
† Universität Heidelberg.
‡ University of Warwick.

(1) Comba, P.; Kerscher, M.; Merz, M.; Müller, V.; Pritzkow, H.; Remenyi, R.; Schiek, W.; Xiong, Y. *Chem.−Eur. J.* **2002**, *8*, 5750.
(2) Comba, P.; Schiek, W. *Coord. Chem. Rev.* **2003**, *238−239*, 21.
(3) Comba, P.; Kerscher, M. *Cryst. Eng.* **2004**, *6*, 197.
(4) Comba, P.; Kerscher, M.; Schiek, W. *Prog. Inorg. Chem.* **2007**, *55*, 613.
(5) Comba, P.; Kerscher, M. *Models, Mistery and Magic of Molecules*; Boeyens, J. C. A., Ogilvie, J., Eds.; Springer: New York, 2008; p 391.
(6) Born, K.; Comba, P.; Ferrari, R.; Kuwata, S.; Lawrance, G. A.; Wadepohl, H. *Inorg. Chem.* **2007**, *46*, 458.
(7) Anastasi, A.; Comba, P.; McGrady, J.; Lienke, A.; Rohwer, H. *Inorg. Chem.* **2007**, *46*, 6420.
(8) Bautz, J.; Comba, P.; Lopez de Laorden, C.; Menzel, M.; Rajaraman, G. *Angew. Chem., Int. Ed.* **2007**, *46*, 8067.
(9) Comba, P.; Lang, C.; Lopez de Laorden, C.; Muruganantham, A.; Rajaraman, G.; Wadepohl, H.; Zajaczkowski, M. *Chem.−Eur. J.* **2008**, *14*, 5313.

10.1021/ic8011052 CCC: $40.75 © 2008 American Chemical Society
Published on Web 09/24/2008

Chart 1

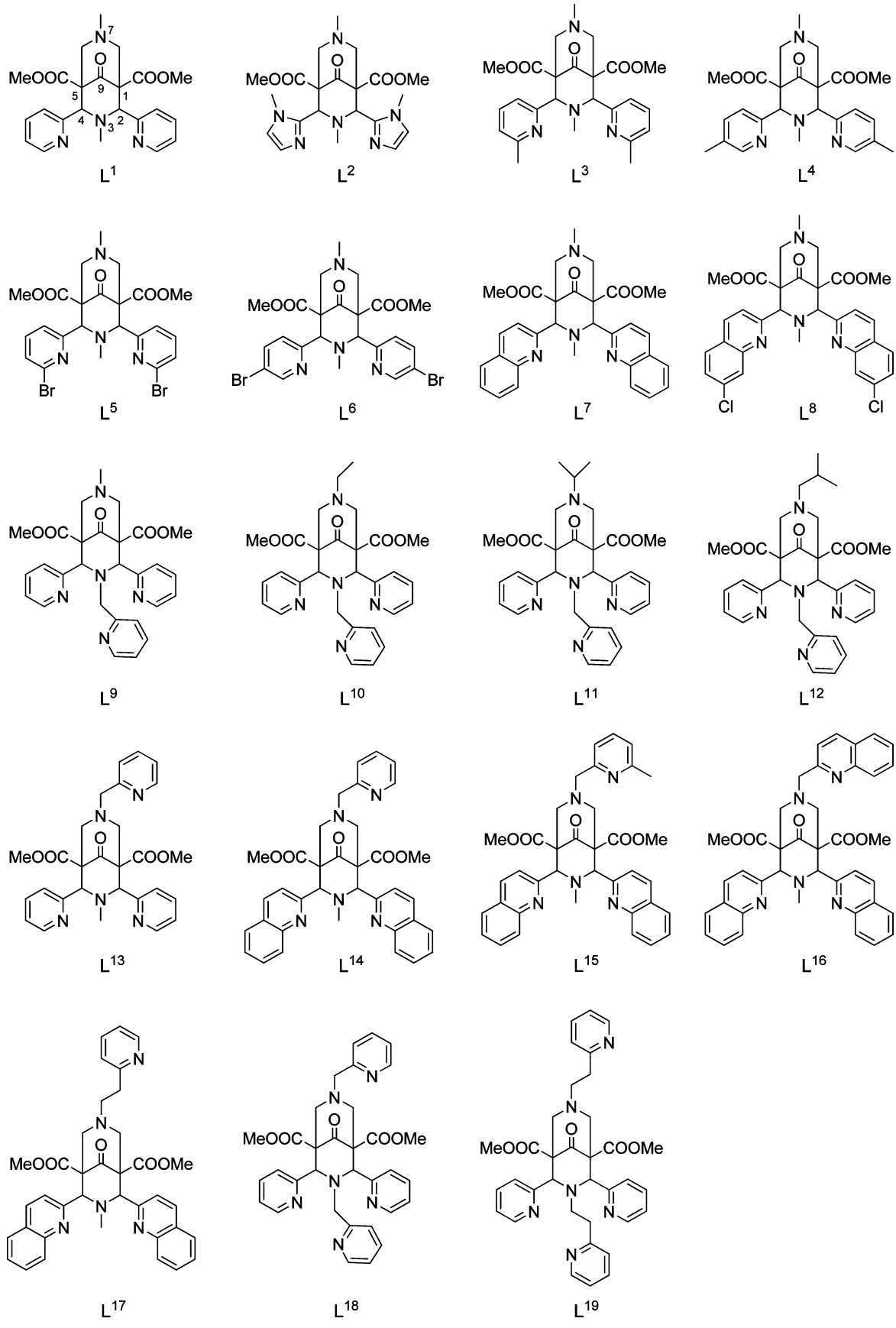

from linear combinations of the Q_θ and Q_ε vibrational modes of the parent octahedron, are usually visualized by the well-known "Mexican hat" potential energy surface.[10–12] To first order, all geometries are equienergetic,

but to second order, tetragonal elongation becomes favored, and the tetragonally compressed structures become saddle points.[13]

With bispidine copper(II) complexes, we have isolated and structurally as well as spectroscopically characterized the first molecular systems where various minimum-energy structures are trapped and "Jahn−Teller isomerism" is demonstrated.[14,15] The analysis, based on empirical force field, ligand field, and approximate density functional (DFT) calculations,[16] leads to some understanding of the factors which influence the relative energies of the various minima on the potential energy surface.[15,18] However, while these studies have helped us to thoroughly understand the structural and electronic properties of experimentally well-characterized systems, they do not allow an accurate and efficient prediction of the structures of new systems, an important requirement for the design of novel bispidine copper(II) complexes with well-specified, desired properties.

Molecular mechanics (MM) modeling can reliably predict molecular structures and the corresponding molecular properties for coordination complexes.[19−21] For Jahn−Teller-active systems such as copper(II), a number of approaches have been adopted, and on the basis of certain approximations, they are generally able to predict structural properties reasonably well, especially for asymmetric ligand systems.[21−24] This has also been confirmed for bispidine copper(II) complexes.[1,6,15,25] However, there are severe restrictions to these approaches, and for complex systems, such as those described here, it is impossible to correctly describe the entire potential energy surface and accurately predict the correct structure with classical MM methods.[26]

The development of a molecular mechanics model for transition metal complexes which includes a ligand-field-based energy term (ligand field molecular mechanics, LFMM) together with the usual functions to describe preferences and penalties for bonds, valence and torsional angles, and nonbonded interactions has been shown to have the potential to accurately predict the structures of metal complexes without assumptions about the type of distortion and with simple and constant parameter sets.[27−30] LFMM is an extension of conventional molecular mechanics, where the "native" M−L stretch and M−L−M angle bend terms are replaced with Morse functions and L−L repulsion terms, respectively. In addition, the torsional force constants involving the metal center (A−M−L−B) are set to zero. The only "conventional" terms remaining which explicitly contain a metal contribution are the M−L−A angle bending potentials plus nonbonding interactions. The latter are treated "normally", that is, using whatever protocol is appropriate for the native force field. The major extra term is the ligand field energy. This comprises two contributions—the classical ligand field stabilization energy (LFSE) and the spin-pairing energy. The latter is only required for low-spin complexes and therefore does not apply to the present copper(II) species. The LFSE is derived from the d-orbital energies computed via the angular overlap model (AOM). The AOM parameters model the M−L σ and π interactions via the e_σ and e_π parameters—for example, $\Delta_{oct} = 3e_\sigma - 4e_\pi$. They are assumed to vary as some inverse power of the bond length. The configurational mixing between the metal valence s orbital and the appropriate d function is also considered via a distance-dependent e_{ds} parameter. The ligand field energy and its gradients are directly incorporated into the optimization. Full details of the LFMM implementation into the Molecular Operating Environment have been published previously.[30] Applications of LFMM include spin-crossover systems,[31] systems where trans-influences lead to specific structural effects[31] and Jahn−Teller-active copper(II) systems.[26,32] Because the bispidine copper(II) complexes described here comprise a unique set of structures where up to three fundamentally different geometries may be stabilized as a function of the coligand or subtle modifications of the ligand backbone, LFMM modeling of the complete set of bispidine copper(II) complexes was considered to be a thorough test for the model and, if successful, would be a useful tool for the accurate prediction of new copper(II) bispidines complexes.

Results and Discussion

The crystallographically determined molecular structures of the copper(II) complexes of 19 different tetra-, penta-, and hexadentate bispidine ligands (see Chart 1) with various monodentate coligands ($X = OH_2$, NCMe, Cl^-, CN^-, NO_3^-) have been determined (not included are structures of dinucleating ligands); experimental and calculated structural

(10) Jahn, H. A.; Teller, E. *Proc. Roy. Soc.* **1937**.
(11) Bersuker, I. B. *Chem. Rev.* **2001**, *101*, 1067.
(12) Figgis, B. N.; Hitchman, M. A. *Ligand Field Theory and its Applications*; Wiley-VCH: Weinheim, Germany, 2000; p 354.
(13) Deeth, R. J.; Hitchman, M. A. *Inorg. Chem.* **1986**, *25*, 1225.
(14) Comba, P.; Hauser, A.; Kerscher, M.; Pritzkow, H. *Angew. Chem., Int. Ed.* **2003**, *42*, 4536; *Angew. Chem.* **2003**, *115*, 4675.
(15) Comba, P.; Martin, B.; Prikhod'ko, A.; Pritzkow, H.; Rohwer, H. *C. R. Chim.* **2005**, *6*, 1506.
(16) Although there is concern that DFT is unable to correctly deal with the Jahn−Teller problem of copper(II) (the Born−Oppenheimer approximation is not valid in the vibronic coupling domain),[11,17] it seems that for structural modeling there generally is no problem.[18]
(17) Bersuker, I. B. *J. Comput. Chem.* **1997**, *18*, 260.
(18) Atanasov, M.; Comba, P.; Martin, B.; Müller, V.; Rajaraman, G.; Rohwer, H.; Wunderlich, S. *J. Comput. Chem.* **2006**, *27*, 1263.
(19) Comba, P. *Coord. Chem. Rev.* **1999**, *182*, 343.
(20) Comba, P.; Hambley, T. W. *Molecular Modeling of Inorganic Compounds*; 2nd ed., with a Tutorial, based on MOMEClite; Wiley-VCH: Weinheim, Germany, 2001.
(21) Comba, P.; Remenyi, R *Coord. Chem. Rev.* **2003**, *238−239*, 9.
(22) Comba, P.; Zimmer, M. *Inorg. Chem.* **1994**, *33*, 5368.
(23) Bol, J. E.; Buning, C.; Comba, P.; Reedijk, J.; Ströhle, M. *J. Comput. Chem.* **1998**, *19*, 512.
(24) Sabolovic, J.; Liedl, K. R. *Inorg. Chem.* **1999**, *38*, 2764.
(25) Bleiholder, C.; Börzel, H.; Comba, P.; Ferrari, R.; Heydt, A.; Kerscher, M.; Kuwata, S.; Laurenczy, G.; Lawrance, G. A.; Lienke, A.; Martin, B.; Merz, M.; Nuber, B.; Pritzkow, H. *Inorg. Chem.* **2005**, *44*, 8145.
(26) Deeth, R. J.; Hearnshaw, L. J. A. *J. Chem. Soc., Dalton Trans.* **2005**, 3638.
(27) Burton, V. J.; Deeth, R. J.; Kemp, C. M.; Gilbert, P. J. *J. Am. Chem. Soc.* **1995**, *117*, 8407.
(28) Burton, V. J.; Deeth, R. J. *J. Chem. Soc., Chem. Commun.* **1995**, 573.
(29) Deeth, R. J. *Coord. Chem. Rev.* **2001**, *212*, 11.
(30) Deeth, R. J.; Fey, N.; Williams-Hubbard, B. J. *J. Comput. Chem.* **2005**, *26*, 123.
(31) Deeth, R. J.; Munslow, I. J.; Paget, V. J. *Molecular Modeling and Dynamics of Bioinorganic Systems*; Banci, L., Comba, P, Eds.; Kluwer: Dordrecht, The Netherlands, 1997; p 77.
(32) Deeth, R. J.; Hearnshaw, L. J. A. *J. Chem. Soc., Dalton Trans.* **2006**, 1092.

parameters are compared in Table 1, and structural plots from the X-ray diffraction experiments appear in Figure 1. In Table 1, the labels N3 and N7 refer to the amines at positions 3 and 7, respectively (see Chart 1, L^1), ar1 and ar2 are the unsaturated nitrogen donors attached at positions 2 and 4, ar3 is the additional pyridyl donor of pentadentate ligands, and X is one or two monodentate donors or the sixth pyridyl group for L^{18}. For six-coordinate complexes, the positions of the X and ar3 groups relative to N3 and N7 are indicated in the table. Table 2 records the LFMM energies, with the bold figure corresponding to the crystallographically observed isomer.

There are eight tetradentate ligands (L^1 through L^8), where the monodentate coligand may be trans to N3 (in-plane with the aromatic amines) or trans to N7. Ligands L^9 through L^{17} are pentadentate with an additional pyridyl substituent attached to N3 (L^9 through L^{12}) or N7 (L^{13} through L^{17}). The remaining two ligands are hexadentate with pyridyl substituents on both N3 and N7. Although the various aromatic N donors clearly have different bonding properties (pK_a(py) = 5.23, pK_a(im) = 6.99, pK_a(5-Mepy) = 6.00, pK_a(quin) = 4.90) in a first-order parametrization, the same parameters have been used for all of them.[33] Despite this approximation, there are only two complexes, $[Cu(L^3)(NCMe)]^{2+}$ and $[Cu(L^8)(NCMe)_2]^{2+}$, where the crystallographic isomer has a significantly (i.e., greater than 5 kJ mol^{-1}) higher energy than the most stable LFMM structure, although we note that the *structural* comparison between the experimental geometry and the corresponding LFMM structure is good.

For L^3 with relatively bulky methyl groups in the plane of Cu, N3, ar1, and ar2, all three structural forms (elongation along all three Cartesian axes) have been trapped experimentally.[15] Intuitively, the ortho methyl substituents on the pyridyl donors of $[Cu(L^3)(NCMe)]^{2+}$ destabilize the position trans to N3, which is consistent with the chloro and aqua analogues where the "extra" ligand is in contrast to the MeCN complex trans to N7. It is difficult to find fault with the force field since, when this steric interaction is removed, as in the meta-substituted $[Cu(L^4)(NCMe)]^{2+}$ and $[Cu(L^6)(NCMe)]^{2+}$ or the unsubstituted $[Cu(L^1)(Cl)]^+$, the calculated structures place the "fifth" donor trans to N3. However, the X-ray crystal structure of $[Cu(L^3)(NCMe)]^{2+}$ has a $[BF_4]^-$ counteranion trans to N7, which could conceivably lead to a favorable electrostatic interaction which we have not included in the LFMM treatment.

For the quinoline derivative, L^7, an experimental copper(II) structure with a coordinated fluoride trans to N3 has also been reported, suggesting that the coordination of the larger chloride trans to N7 is electronically less favored and enforced by steric effects exerted by the ligand.[34] This is consistent with the calculated data for $[Cu(L^1)(Cl)]^+$ and $[Cu(L^2)(Cl)]^+$, where the steric effects are smaller and chloride coordination trans to N3 is favored. Notwithstanding the comments made above concerning counterions, it could be that the force field is not getting the correct balance between steric and electronic factors for trans N3 versus trans N7 coordination and is favoring the latter too much.

The other LFMM "mistake" is $[Cu(L^8)(NCMe)_2]^{2+}$, although the calculated energy difference between elongation trans to N7 (the X-ray geometry) and elongation along the aromatic amine direction (the LFMM minimum) is only 5 kJ mol^{-1}, just at the somewhat arbitrary significance threshold of 5 kJ mol^{-1}. As a general remark of caution, we also note that, due to crystal lattice effects, the crystal structures do not necessarily represent the minimum on the potential energy surface of the molecular structures. This is of particular importance in cases where the energy differences between various isomers are small, as for the copper−bispidine complexes discussed here, especially also for the system with ligand L^8.

The N3-pyridinemethyl-substituted pentadentate ligands L^9 through L^{12} were the first complexes to display elongations along Cu−N7 and ar1−Cu−ar2.[14] From experimental results, it appeared that, with MeCN as a coligand, the most stable form of the copper(II) complex with the L^9 bispidine ligand has an elongation along the pyridine groups, and with bulkier coligands (Cl^-, OH_2) or substituents at N7 (ethyl or larger instead of methyl), this isomer is destabilized with respect to that with an elongated Cu−N7 bond. The LFMM results concur, although the energetic balance between the two isomers is predicted to be very delicate, with less than 5 kJ mol^{-1} difference in every case. This subtlety is nicely illustrated by the series $[Cu(L^n)(NCMe)]^+$, $n = 9-11$, where the progressive increase in the steric bulk of the N7 alkyl substituent, R, results in a changeover from ar1−Cu−ar2 elongation for L^9 (R = methyl, the smallest substituent) to N7 elongation for L^{11} (R = isopropyl, the largest substituent).

With the ligand L^{13}, where the pyridine group is appended to N7 and is therefore isomeric with L^9, all structures with different coligands have the elongation along Cu−N7,[4,35] except for the trinuclear structure, where a bridging cyanide is coordinated trans to N7 and the ar1−Cu−ar2 axis is elongated.[36] This switch of the Jahn−Teller axis was qualitatively interpreted to be due to the fact that the strong CN^- ligand cannot be on the Jahn−Teller axis; the relatively long bond to N7 in turn is due to a trans influence exerted by CN^-.[4,7,36] The LFMM optimizations for $[Cu(L^{13})(Cl)]^+$ predict virtually equi-energetic forms. Given that there is just the single structure containing isocyanides, no LFMM calculations have been attempted, but the observation of long Cu−N7 and Cu−ar bonds could also be consistent with both minima being occupied in the solid state.

The derivatives L^{14} through L^{16} with bulkier aromatic donor groups lead to a destabilization of the isomer with a Cu−N7 elongation, and all have a minimum energy structure with elongated ar1−Cu−ar2 axes. The LFMM calculations are consistent with experimental results in that only one

(33) This clearly leads to larger than usual error limits, but the aim of this paper only was to validate the approach.
(34) Comba, P.; Lopez de Laorden, C.; Pritzkow, H. *Helv. Chim. Acta* **2005**, *88*, 647.
(35) Comba, P.; Merz, M.; Pritzkow, H. *Eur. J. Inorg. Chem.* **2003**, 1711.
(36) Atanasov, M.; Busche, C.; Comba, P.; El Hallak, F.; Martin, B.; Rajaraman, G.; van Slageren, J.; Wadepohl, H. *Inorg. Chem.* **2008**, *47*, 8112.

Table 1. Experimentally Determined (italics) and Computed Structural Parameters (distances in Å, angles in deg; elongated bonds in bold face) of Bispidinecopper(II) Complexes[a]

	Tetradentate Bispidines										
	[Cu(L^1)-Cl]$^+$	[Cu(L^2)-Cl]$^+$	[Cu(L^3)-Cl]$^+$	[Cu(L^3)-(NCMe)]$^{2+}$	[Cu(L^3)-(OH$_2$)]$^{2+}$	[Cu(L^3)-(NO$_3$)]$^{+d}$	[Cu(L^4)-(NCMe)]$^{2+}$	[Cu(L^5)-(NCMe)$_2$]$^{2+}$	[Cu(L^6)-(NCMe)]$^{2+}$	[Cu(L^7)-Cl]$^+$	[Cu(L^8)-(NCMe)$_2$]$^{2+}$
	Distances										
Cu−N3	*2.042(3)* 2.04 [2.11]	*2.115(2)* 2.10	***2.147(3)*** **2.14** [2.02]	*2.005(4)* **2.12** [2.03]	***2.132(2)*** **2.09** [2.02]	*1.976(1)*, *1.987(2)* 2.11 [2.05]	*2.007(1)* 2.03	*2.050(4)* 2.11 [2.05]	*2.010(5)* 2.03	**2.149(1)**, ***2.143(2)*** **2.13** [2.05]	*1.987(1)* 2.11 [2.04]
Cu−N7	***2.273(3)*** **2.32** [2.24]	**2.316(2)** **2.36**	*2.120(3)* 2.21 **[2.42]**	***2.376(4)*** 2.18 **[2.34]**	*2.079(1)* 2.21 **[2.31]**	*2.092(2)*, *2.032(2)* 2.18 **[2.35]**	***2.244(1)*** **2.30**	*2.103(6)* 2.18 [2.36]	***2.256(5)*** **2.30**	*2.131(2)*, *2.135(2)* 2.22 **[2.45]**	***2.370(2)*** 2.18 **[2.39]**
Cu−ar1	*2.020(3)* 2.08 [2.04]	*1.967(2)* 2.00	*2.061(3)* 2.04 [2.11]	*2.052(4)* 2.02 [2.07]	*2.016(1)* 2.02 [2.07]	***2.259(2)***, ***2.377(3)*** **2.30** [2.13]	*1.991(1)* 2.02	**2.395(4)** **2.31** [2.13]	*2.022(4)* 2.02	*2.004(2)*, *2.017(2)* 2.04 [2.09]	*2.124(1)* **2.33** [2.11]
Cu−ar2	*2.024(3)* 2.08 [2.04]	*1.971(2)* 2.00	*2.064(3)* 2.04 [2.12]	*2.075(4)* 2.02 [2.07]	*2.037(1)* 2.02 [2.07]	***2.347(2)***, ***2.376(2)*** **2.30** [2.13]	*2.007(1)* 2.02	**2.441(5)** **2.31** [2.13]	*2.020(4)* 2.02	*2.019(2)*, *2.033(2)* 2.05 [2.09]	*2.090(1)* **2.33** [2.11]
Cu−X	*2.232(1)*[b] 2.23 [2.25]	*2.228(6)*[b] 2.17	*2.221(2)*[b] 2.28[b] [2.24][c]	*1.951(4)*[c] 2.07[b] [2.00][c]	*1.979(1)*[c] *2.04*[b] [1.98] [c]	*1.964(2)*, *1.982(2)*[c] *2.283(2)*, *2.139(2)*[b] 2.04 [2.03][c] 2.11 **[2.60]**[b]	*1.965(1)*[c] 1.98[c]	*1.985(4)*[c] *2.051(6)*[b] 2.05;[c] [2.04][c] 2.09;[b] [2.57][b]	*1.957(5)*; 1.98	***2.265(1)***, ***2.255(1)*** **2.28**[b][2.25][b]	*1.967(1)*[c] **2.634(2)**[b] 2.07[c] 2.08 [b] [2.08][c] **[2.62]**[b]
N3···N7	*2.921(4)* 2.98 [2.97]	*2.917(2)* 2.98	*2.930(5)* 2.99 [3.01]	*2.934(6)* 2.99 [3.00]	*2.927(2)* 2.97 [2.99]	*2.853(2)*, *2.834(2)* 2.95 [3.00]	*2.905(2)* 2.99	*2.844(7)* 2.94 [2.99]	*2.921(7)* 2.99	*2.922(2)*, *2.913(2)* 2.99 [3.02]	*2.919(2)* 2.94 [3.00]
ar1···ar2	*3.971(4)* 4.11 [4.05]	*3.869(3)* 3.95	*4.084(5)* 4.06 [4.10]	*4.034(6)* 4.01 [4.04]	*4.020(2)* 4.01 [4.07]	*4.501(2)*, *4.618(3)* 4.47 [4.19]	*3.938(2)* 3.99	*4.650(6)* 4.48 [4.19]	*3.970(6)* 3.99	*3.992(2)*, *4.016(2)* 4.07 [4.03]	*4.124(2)* 4.50 [4.15]
	Angles										
N3−Cu−N7	*85.02(9)* 86 [86]	*82.20(6)* 84	*86.71(12)* 87 [84]	*83.66(14)* 88 [87]	*88.05(5)* 88 [87]	*89.00(6)*, *89.69(7)* 87 [86]	*86.03(4)* 87	*86.4(2)* 86 [85]	*86.2(2)* 87	*86.11(6)*, *85.86(6)* 87 [84]	*83.61(5)* 86 [85]
N3−Cu−ar1	*81.25(10)* 82 [83]	*80.58(7)* 82	*81.62(13)* 84 [81]>	*80.92(16)* 83 [82	*83.32(5)* 84 [83]	*80.37(5)*, *77.79(7)* 78 [82]	*82.45(4)* 84	*76.2(2)* 78 [82]	*81.9(2)* 84	*82.92(6)*, *82.52(7)* 84 [81]	*79.33(6)* 77 [82]
N3−Cu−ar2	*81.15(10)* 82 [83]	*80.51(7)* 82	*82.38(12)* 84 [81]	*81.49(15)* 84 [82]	*82.79(5)* 84 [83]	*78.72(6)*, *78.37(7)* 78 [82]	*82.25(4)* 83	*75.5(2)* 77 [82]	*81.3(2)* 84	*82.80(6)*, *82.63(6)* 84 [81]	*81.67(6)* 77 [82]
ar1−Cu−ar2	*158.13(10)* 161 [166]	*158.58(7)* 161	*163.82(13)* 167 [151]	*155.62(16)* 164 [156]	*165.43(5)* 167 [158]	*155.60(6)*, *152.55(8)* 153 [161]	*159.97(4)* 163	*148.2(1)* 152 [160]	*158.4(2)* 163	*165.70(6)*, *165.05(7)* 168 [149]	*156.31(6)* 151 [159]
N3−Cu−X	*165.02* 166 [124]	*166.69(5)* 164	*112.97(9)* 110 [178]	*174.32(17)* 108 [179]	*110.18(6)* 112 [178]	*171.33(6)*, *169.66(7)* *111.39(7)*, *106.89(7)* 177 [177] 96 [98]	*168.40(4)* 171	*178.2(2)*, *95.9(2)* 177, 97 [175], [100]	*172.3(2)* 171	*109.20(4)*, *109.88(5)* 110 [176]	*169.93(6)*, *100.58(5)* 176, 97 [176], [99]

	Penta- and Hexadentate Bispidines											
	[Cu(L^9)-Cl]$^+$	[Cu(L^9)-(NCMe)]$^{2+}$	[Cu(L^{10})-(NCMe)]$^{2+}$	[Cu(L^{11})-(NCMe)]$^{2+}$	[Cu(L^{12})-(OH$_2$)]$^{2+}$	[Cu(L^{13})-Cl]$^+$	[Cu(L^{14})-Cl]$^+$	[Cu(L^{15})-(Cl)	[Cu(L^{16})-(NCMe)]$^{2+}$	[Cu(L^{17})]$^{2+}$	[Cu(L^{18})]$^{2+}$	[Cu(L^{19})]$^{2+}$
	Distances											
Cu−N3	*2.070(2)* 2.08 [2.09]	*2.105(2)* 2.06 [2.07]	*2.063(5)* 2.07 [2.09]	*2.056(3)* 2.02 [2.02]	*2.031(2)* 2.11 [2.11]	*2.036(2)* 2.12 [2.20]	*2.0888(14)* 2.18	*2.159(3)* 2.21	*2.122(2)* 2.14	*1.953(2)* 2.01	*2.093(3)*, *2.087(3)* 2.07 [2.07]	*2.016(2)* 2.02
Cu−N7	***2.479(2)*** **2.45** [2.30]	*2.106(2)* 2.17 [**2.35**]	**2.472(5)** **2.39** [2.20]	**2.604(3)** **2.42** [2.22]	**2.466(2)** **2.34** [2.20]	**2.368(2)** **2.37** [2.16]	*2.1142(15)* 2.17	*2.079(3)* 2.16	*2.015(2)* 2.13	*2.095(2)* **2.21**	*2.038(3)*, *2.045(3)* **2.11 [2.32]**	***2.195(3)*** **2.26**
Cu−ar1	*2.012(2)* 2.10 [**2.23**]	**2.260(2)** **2.22** [2.02]	*1.992(5)* 2.04 [**2.24**]	*2.003(2)* 2.02 [**2.22**]	*1.992(2)* 2.02 [**2.17**]	*2.028(2)* 2.04 [**2.27**]	**2.3449(15)** **2.32**	**2.686(3)** **2.42**	***2.931(3)*** **2.40**	***2.311(2)*** **2.21**	**2.608(3)**, **2.280(3)** 2.23 [2.03]	*2.024(2)* 2.04
Cu−ar2	*1.987(3)* 2.09 [**2.22**]	**2.353(2)** **2.22** [2.02]	*1.996(5)* 2.02 [**2.22**]	*2.001(2)* 2.04 [**2.24**]	*1.983(2)* 2.03 [**2.19**]	*2.029(2)* 2.01 [**2.23**]	**2.6093** **2.41**	***2.320(3)*** **2.29**	***2.288(2)*** **2.31**	***2.269(2)*** **2.19**	*2.262(3)*, ***2.573(3)*** 2.28 [2.04]	*2.006(2)* 2.04
Cu−ar3	**2.544(3)** **2.25** [2.15]	*2.027(2)* 2.06 [2.18]	**2.279(6)** **2.20** [2.06]	***2.289(3)*** **2.21** [2.06]	***2.499(2)*** 2.15 [2.05]	*2.029(2)* 2.17 [2.15]	*2.0192(15)* 2.13	*2.159(3)* 2.27	*2.108(2)* 2.17	*1.927(2)* 1.99	*2.031(3)*, *2.009(3)*[c] 2.07 [2.07]	*1.967(2)*[c] 2.01
Cu−X	*2.255(1)*[c]	*2.015(2)*[c]	*2.022(6)*[c]	*2.014(3)*	*1.958(2)*	**2.717(1)**	*2.3054(5)*	*2.264(1)*	*1.987(2)*		*2.013(3)*, *2.028(3)*[b]	

Table 1. Continued

	Penta- and Hexadentate Bispidines										
	$[Cu(L^9)-Cl]^+$	$[Cu(L^9)-(NCMe)]^{2+}$	$[Cu(L^{10})-(NCMe)]^{2+}$	$[Cu(L^{11})-(NCMe)]^{2+}$	$[Cu(L^{12})-(OH_2)]^{2+}$	$[Cu(L^{13})-Cl]^+$	$[Cu(L^{14})-Cl]^+$	$[Cu(L^{15})-(Cl)$	$[Cu(L^{16})-(NCMe)]^{2+}$	$[Cu(L^{17})]^{2+}$	$[Cu(L^{18})]^{2+}$	$[Cu(L^{19})]^{2+}$
	2.27 [2.25]	2.06 [2.11]	2.09[c] [2.07][c]	2.10 [2.09]	2.12 [2.08]	**2.54** [2.28]	2.29	2.25	2.04		2.06 [**2.22**]	
N1···N2	*2.931(3)*	*2.884(2)*	*2.975(7)*	*3.016(5)*	2.931(3)	*2.915(3)*	*2.853(2)*	*2.836(4)*	*2.816(4)*	*2.834(3)*	*2.841(4)*, *2.830(4)*	*2.903(3)*
	3.02 [2.98]	2.95 [3.02]	3.04 [2.97]	3.07 [3.00]	3.04 [2.99]	3.00 [2.95]	2.96	2.95	2.91	2.97	2.92 [3.01]	3.01
ar1···ar2	*3.966(3)*	*4.508(3)*	*3.954(7)*	*3.971(3)*	*3.949(3)*	*3.995(2)*	*4.795(2)*	*4.821(5)*	*4.969(4)*	*4.464(3)*	*4.696(5)*, *4.671(4)*	*3.958(3)*
	4.15 [4.36]	4.35 [4.02]	4.04 [4.36]	4.04 [4.36]	4.12 [4.28]	4.02 [4.36]	4.58	4.55	4.55	4.34	4.41 [4.04]	4.04
						Angles						
N3−Cu−N7	*79.690(8)*	*86.44(6)*	*81.5(2)*	*79.73(9)*	*80.73(6)*	*82.53(6)*	*85.51(6)*	*84.00(11)*	*85.77(9)*	*88.80(8)*	*86.90(12)*, *86.45(12)*	*87.04(8)*
	83 [85]	86 [86]	86 [88]	86 [88]	86 [88]	84 [85]	86	85	86	89	89 [86]	89
N3−Cu−ar1	*83.63(9)*	*78.38(6)*	*82.7(2)*	*82.27(11)*	*84.09(7)*	*81.39(7)*	*76.58(5)*	*73.07(10)*	*68.04(8)*	*78.63(8)*	*72.80(11)*, *78.25(11)*	*82.29(8)*
	83 [80]	80 [84]	84 [79]	83 [79]	83 [80]	83 [77]	77	75	75	81	78 [83]	84
N3−Cu−ar2	*81.74(10)*	*77.71(7)*	*82.4(2)*	*83.26(11)*	*82.95(7)*	*80.94(7)*	*74.68(5)*	*75.91(10)*	*77.49(9)*	*80.07(8)*	*78.54(11)*, *72.98(11)*	*82.15(9)*
	82 [79]	80 [84]	83 [79]	84 [79]	83 [80]	82 [76]	76	77	78	83	80 [85]	83
ar1−Cu−ar2	*165.37(10)*	*155.49(6)*	*165.1(2)*	*165.39(11)*	*167.00(8)*	*160.07(7)*	*150.84(5)*	*148.70(10)*	*144.09(7)*	*154.18(7)*	*149.21(11)*, *148.53(11)*	*158.32(9)*
	164 [157]	158 [167]	166 [156]	167 [157]	166 [158]	165 [151]	151	150	150	161	156 [166]	163
N7−Cu−ar3	*155.10(8)*	*169.99(7)*	*161.9(2)*	*158.91(9)*	*158.85(6)*	*79.27(7)*	*83.29(6)*	*83.46(11)*	*83.76(9)*	*100.95(8)*	*171.36(13)*, *172.13(13)*	
	164 [169]	173 [169]	168 [172]	168 [172]	169 [172]	77 [81]	82	81	83	98	171 [166]	
N3−Cu−X	*173.81(7)*	*175.78(8)*	*178.5(2)*	*176.62(12)*	*172.89(7)*	*105.30(5)*	*97.36(4)*	*93.76(8)*	*95.22(9)*		*153.31(12)*, *154.39(12)*	*171.35(9)* *174*
	179 [178]	178 [179]	177 [172]	176 [172]	177 [175]	102 [102]	99	97	95		165 [165]	

[a] The nomenclature is that of Chart 1 and Figure 1; references of published structures are those given in Figure 1; square brackets refer to parameters from the less-stable LFMM structures given in Table 2. [b] Trans to N7. [c] Trans to N3. [d] The structure of L^3-NO_3 was modeled as $L^3-(NCMe)_2$. [e] Parameters used for CN^- were those also used for MeCN.

stable isomer can be located. However, the extent of the ar1−Cu−ar2 elongation is computed to be rather less than observed. Thus, while the LFMM gets the correct sense and asymmetry of elongation, the longer of the two Cu−ar contacts is predicted to be several tenths of an ångstrom shorter than the X-ray value.

Of particular interest is ligand L^{17}, a derivative of L^{14} with an ethylene- instead of methylene-linked N7-appended pyridine group. The structure of the L^{17}-based copper(II) complex has an elongation along ar1−Cu−ar2, extremely short bonds to N3 and ar3, and a moderately short bond to N7 but, unexpectedly, no coligand on the in-plane site trans to N7.[34] The structure of $[Cu(L^{14})(Cl)]^+$ is qualitatively similar but has a chloride trans to N7. Significantly, the structural changes between $[Cu(L^{17})]^{2+}$ and $[Cu(L^{14})(Cl)]^+$ are quite well reproduced by LFMM. For example, relative to $[Cu(L^{14})(Cl)]^+$, for $[Cu(L^{17})]^{2+}$, the experimental Cu−N3, Cu−ar3, Cu−ar1, and Cu−ar2 decrease by 0.14, 0.09, 0.04, and 0.34 Å, respectively, while Cu−N7 hardly changes. The corresponding LFMM values are 0.17, 0.14, 0.09, and 0.22 Å.

The hexadentate ligands L^{18} and L^{19} are interesting in that the former is six-coordinate and ar1−Cu−ar2 elongated, while the latter is five-coordinate and Cu−N7 elongated. Moreover, LFMM calculations for the six-coordinate L^{19} complex (not shown in Tables 1 and 2) also give an N7 elongated structure with the other isomer some 13.5 kJ mol^{-1} higher in energy. The elongation of the bond to the donor trans to N7 has previously been interpreted as the result of steric repulsion of the "long" pyridine group.[37] The LFMM calculations show that the total van der Waals energy of the penta-coordinated complex is reduced by 30 kJ mol^{-1}; plus there is an additional reduction in torsional strain of about 20 kJ mol^{-1}. While these numbers refer to the entire complex and should be interpreted with caution since the molecular connectivities are different, theory does seem to provide some support for the previous analysis.

The general performance of the LFMM force field can be assessed by comparing observed and calculated Cu−L bond lengths for all the complexes. The Cu−L bond length root mean square (rms) deviations for nine complexes are 0.05 Å or less, with 20 reproduced to a rms derivation of 0.1 Å or less. Across all of the complexes, the Cu−amine and Cu−pyridyl bond length rms derivations are 0.07 and 0.12 Å, respectively. These results are visualized in Figure 2, which is a plot of the computed versus experimentally observed Cu−L distances; for $[Cu(L^3)(Cl)]^+$ and $[Cu(L^8)(NCMe)]^{2+}$, the less stable structures which represent those observed by experimentation have been selected.

Although the correlations between theory and experiment are generally good with R^2 values usually greater than 0.8, the slopes of the trendlines are consistently below 1, indicating that the FF is systematically too "stiff". The Cu−N7 bonds tend in general to be predicted a little bit too long unless these bonds correspond to the Jahn−Teller axis. This seems to be a specific problem related to the bispidine

(37) Comba, P.; Kerscher, M.; Lawrance, G. A.; Martin, B.; Wadepohl, H.; Wunderlich, S. *Angew. Chem., Int. Ed.* **2008**, *47*, 4734.

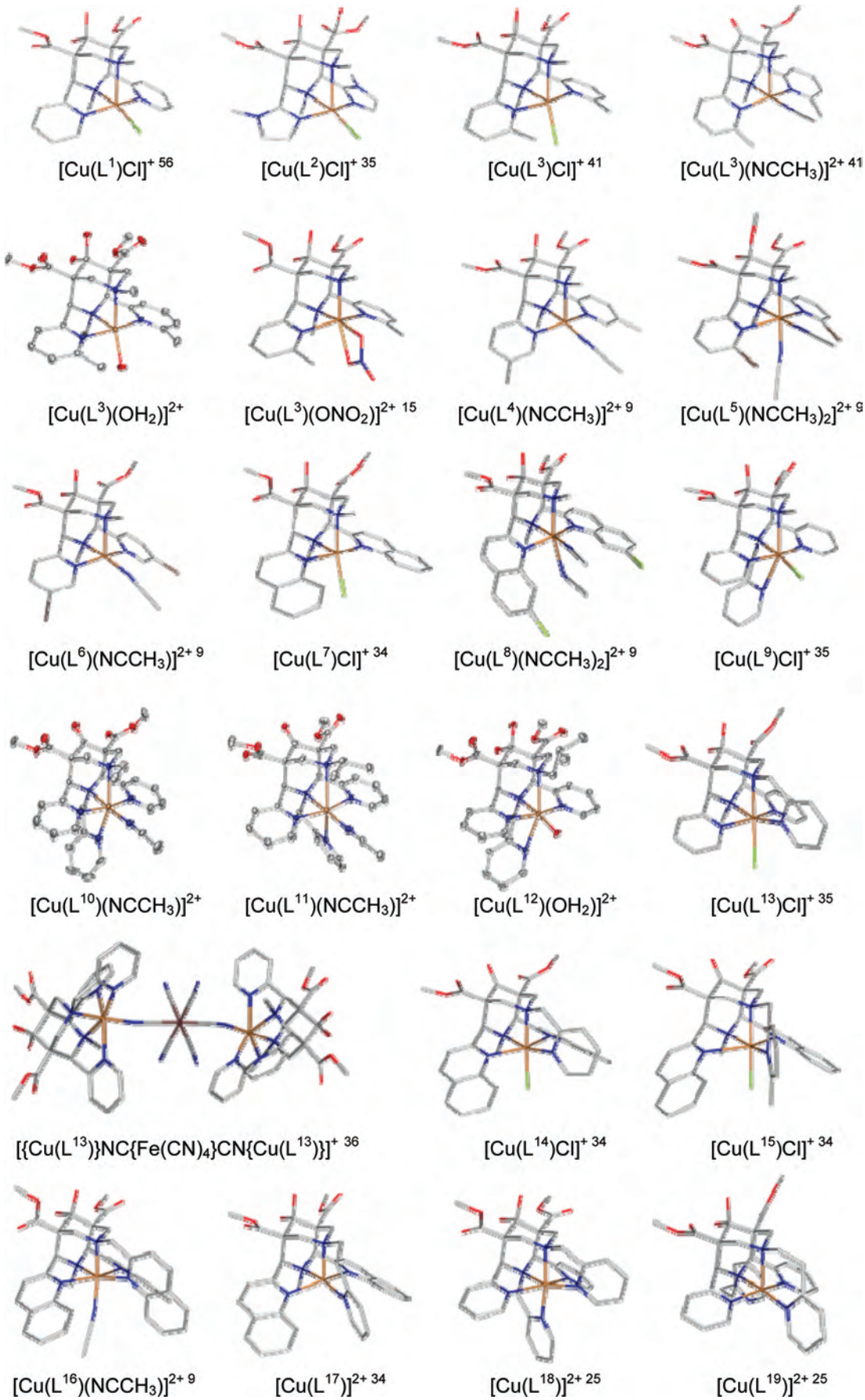

Figure 1. Experimental structures of bispidine copper(II) complexes. New structures are presented as ORTEP ellipsoids (50% ellipsoid probability), and previously published structures are given in a stick presentation; the nomenclature is that of Chart 1 and that used in Tables 1 and 2.

Table 2. Computed Relative Energies (kJ/mol) of the Various Isomers of the Bispidine−Copper(II) Complexes of Table 1 (The Nomenclature Is That of Chart 1 and Is That Used in Table 1 and Figure 1)[a,b,c]

	pentacoordinate complexes		hexacoordinate complexes		
tetradentate bispidines	coligand trans to N3	coligand trans to N7	elongation Cu−N3	elongation Cu−N7	elongation ar1−Cu−ar2
$[Cu(L^1)(Cl)]^+$	**−398.5**	−390.5			
$[Cu(L^2)(Cl)]^+$	**−534.6**	NoMin			
$[Cu(L^3)(Cl)]^+$	−298.3	**−348.2**			
$[Cu(L^3)(NCMe)]^{2+}$	**−423.6**	−437.4			
$[Cu(L^3)(OH_2)]^{2+}$	−378.8	**−389.7**			
$[Cu(L^3)(NCMe)_2]^{2+}$ [d]			NoMin	−469.7	**−472.6**
$[Cu(L^4)(NCMe)]^{2+}$	**−347.4**	NoMin			
$[Cu(L^5)(NCMe)_2]^{2+}$			NoMin	−393.9	**−398.9**
$[Cu(L^6)(NCMe)]^{2+}$	**−380.5**	NoMin			
$[Cu(L^7)(Cl)]^+$	−187.7	**−248.9**			
$[Cu(L^8)(NCMe)_2]^{2+}$			NoMin	**−257.3**	−262.3
penta- and hexadentate bispidines	pentacoordinate complexes		hexacoordinate complexes		
	coligand trans to N3	coligand trans to N7	elongation Cu−N3	elongation Cu−N7	elongation ar1−Cu−ar2
$[Cu(L^9)(Cl)]^+$			NoMin	**−427.4**	−427.0
$[Cu(L^9)(NCMe)]^{2+}$			NoMin	−433.7	**−435.8**
$[Cu(L^{10})(NCMe)]^{2+}$			NoMin	**−471.0**	−471.4
$[Cu(L^{11})(NCMe)]^{2+}$			NoMin	**−406.4**	−403.1
$[Cu(L^{12})(OH_2)]^{2+}$			NoMin	**−340.6**	−338.6
$[Cu(L^{13})Cl]^+$			NoMin	**−435.3**	−435.8
$[Cu(L^{14})Cl]^+$			NoMin	NoMin	**−381.7**
$[Cu(L^{15})Cl]^+$			NoMin	NoMin	**−323.5**
$[Cu(L^{16})(NCMe)]^{2+}$			NoMin	NoMin	**−194.8**
$[Cu(L^{17})]^{2+}$	−179.8	NA			
$[Cu(L^{18})]^+$			NoMin	−445.8	**−450.8**
$[Cu(L^{19})]^{2+}$	−344.0	NA			

[a] Entries in boldface indicate the X-ray crystal structure geometry. [b] NoMin implies attempts to locate the relevant structure collapsed to one of the other minima. [c] Ligand geometry precludes fifth donor trans to N7. [d] Model for $[Cu(L^3)(NO_3)]^+$, see Table 1 and text.

ligands and has also been observed with conventional force field structure optimizations.[1,6,25,38] In contrast, the Cu−N3 bond lengths agree well with experimental results, providing the comparison is limited to five-coordinate complexes. The scatter for six-coordinate species is much greater. For Cu−N7, Cu−ar1, and Cu−ar2, there are clear clusters of points at shorter bond lengths with a discernible gap to systems with longer bond lengths, which is consistent with the Jahn−Teller distortions. That is, we anticipate the bond length either being short or long rather than spanning all values from short through long. For the other bond, there is again the "clump" of values around 2.1 Å with a wide spread of longer distances.

An interesting observation is that, in the original study on bispidine−copper(II)-based Jahn−Teller isomers with ligands based on L^9, there was no indication of dynamic behavior; that is, a variation of temperature in the range of 4−300 K did not lead to the expected switching from one to another isomer.[14] Preliminary computational tests indicate that, as expected, the computed energy barrier between the two minimum structures is small. The selective stabilization of one of the three isomers in the examples which were thoroughly studied experimentally could thus be due to large differences in the free energy rather than high energy barriers between nearly degenerate minima (note that a difference of more than approximately 10 kJ/mol leads to full selectivity). Alternatively, the force field may require further refinement. We already noted the calculated changeover from ar1−Cu−ar2 elongation in $[Cu(L^9)(NCMe)]^+$ through near degeneracy in $[Cu(L^{10})(NCMe)]^+$ to N7 elongation in $[Cu(L^{11})(NCMe)]^+$ and correlated this with the steric effect of the N7 substituent, just as in the study mentioned above.[14] Thus, the force field predicts the correct *sense* of relative energies but may perhaps be underestimating the *magnitude* of the differences. Further parameter development, ideally using automated methods,[39] might improve matters. Moreover, the lack of explicit electrostatic interactions and environmental effects could conceivably be problematic, and the prediction of the most stable isomer has to be interpreted with care in each case. Nevertheless, the overall performance of the current LFMM approach is generally satisfactory, especially for molecular structures.

Conclusion

LFMM has been shown to be able to predict the structural type of bispidine−copper(II) complexes. This is not a trivial achievement because the potential energy surface of bispidine complexes is relatively flat with various shallow minima. The fact that the isomers strongly differ in their structures and, consequently, in their molecular properties makes the design of bispidine ligands which are able to specifically stabilize certain structures a very valuable task. Steric and electronic influences of the bispidine and mono- or bidentate coligands have been found to be of importance for the

(38) Comba, P.; Kerscher, M.; Roodt, A. *Eur. J. Inorg. Chem.* **2004**, *23*, 4640.

(39) Norrby, P.-O.; Brandt, P. *Coord. Chem. Rev.* **2001**, *212*, 79.

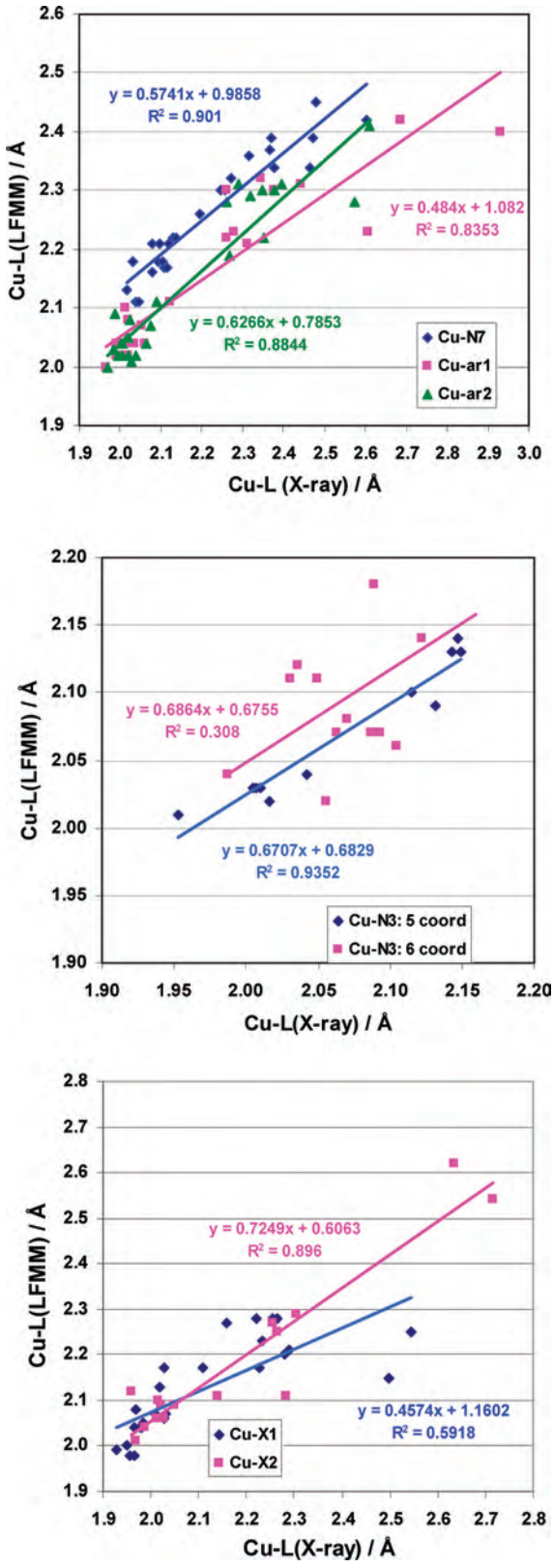

Figure 2. Comparison of observed and calculated copper−ligand bond lengths for bispidine complexes.

stabilization or destabilization of specific isomers, and the LFMM model is able to deal with all of these influences. The parametrization was based on molecular structures, and consequently, it appears that the computed relative energies are not as accurate as we would like. Further development, possibly including explicit electrostatic and environmental effects, seems warranted.

Experimental Section

Syntheses. The ligands and their copper(II) complexes were prepared as described.[9,15,25,34,35,40−44] New ligands (L^{10}, L^{11}, and L^{12}) and complexes ($[Cu(L^3)(OH_2)]^{2+}$, $[Cu(L^{10})(NCCH_3)]^{2+}$, $[Cu(L^{11})(NCCH_3)]^{2+}$, and $[Cu(L^{12})(NCCH_3)]^{2+}$) were prepared in analogy to those already published in acceptable yields (ligands: 19%, 63%, and 25%; complexes: 66%, 73%, and 87%) and fully characterized (NMR, IR, elemental analysis).

Crystal Structure Determination. Crystal data and details of the structure determinations are listed in Table 3. Intensity data were collected at 100 K with a Bruker AXS Smart 1000 CCD diffractometer (Mo Kα radiation, graphite monochromator, λ = 0.71073 Å). Data were corrected for Lorentz, polarization, and absorption effects (semiempirical, SADABS).[45,46] The structures were solved by direct methods with dual-space recycling ("Shake-and-Bake";[47,48] $[Cu(L^3)(OH_2)](ClO_4)_2 \cdot H_2O$ and $[Cu(L^{11})(NCCH_3)](BF_4)_2 \cdot NCCH_3 \cdot 0.5H_2O$), conventional direct methods[46,49] ($[Cu(L^{10})(NCCH_3)](BF_4)_2 \cdot 1.4\ NCCH_3$), or by the heavy atom method combined with structure expansion by direct methods applied to difference structure factors[50,51] ($[Cu(L^{12})(OH_2)](CF_3SO_3)_2 \cdot H_2O$) and refined by full-matrix least-squares methods based on all unique F^2.[46,49] All non-hydrogen atoms were given anisotropic displacement parameters. Hydrogen atoms were generally input at calculated positions and refined with a riding model. Hydrogen atoms of solvent water were placed to maximize hydrogen bonding,[52,53] with atomic charges calculated from partial equalization of orbital electronegativity.[54] When justified by the quality of the data, the positions of some hydrogen atoms (coordinated water in $[Cu(L^3)(OH_2)](ClO_4)_2 \cdot H_2O$ and all water in $[Cu(L^{12})(OH_2)](CF_3SO_3)_2 \cdot H_2O$) were taken from difference Fourier syntheses and refined with appropriate distance restraints. Restraints were also used for the 1,2 and 1,3 distances in the ClO_4^- and BF_4^- anions.

Molecular Mechanics Calculations. All LFMM calculations were carried out using DommiMOE,[30] our extended version of the

(40) Haller, R.; Unholzer, H. *Arch. Pharm.* **1972**, *305*, 855.
(41) Börzel, H.; Comba, P.; Hagen, K. S.; Katsichtis, C.; Pritzkow, H. *Chem.—Eur. J.* **2000**, *6*, 914.
(42) Siener, T.; Cambareri, A.; Kuhl, U.; Engelberger, W.; Haurand, M.; Kögel, B.; Holzgrabe, U. *J. Med. Chem.* **2000**, *43*, 3746.
(43) Börzel, H.; Comba, P.; Hagen, K. S.; Merz, M.; Lampeka, Y. D.; Lienke, A.; Linti, G.; Pritzkow, H.; Tsymbal, L. V. *Inorg. Chim. Acta* **2002**, *337*, 407.
(44) Comba, P.; Seibold, B.; Wadepohl, H. Work in progress.
(45) Sheldrick, G. M. *SADABS-2004−2007*; Bruker AXS: Göttingen, Germany, 2004− 2007.
(46) Sheldrick, G. M. *Acta Crystallogr.* **2008**, A64.
(47) Burla, M. C.; Camalli, M.; Carrozzini, B.; Cascarano, G. L.; Giacovazzo, C.; Polidori, G.; Spagna, R. *SIR2002*; University of Bari: Bari, Italy, 2002.
(48) Burla, M. C.; Camalli, M.; Carrozzini, B.; Cascarano, G. L.; Giacovazzo, C.; Polidori, G.; Spagna, R. *J. Appl. Crystallogr.* **2003**, *36*, 1103.
(49) Sheldrick, G. M. *SHELXL-97*; University of Göttingen: Göttingen, Germany, 1997.
(50) Beurskens, P. T. *Crystallographic Computing 3*; Sheldrick, G. M., Krüger, C., Goddard, R., Eds.; Clarendon Press: Oxford, U.K., 1985; p 216.
(51) Beurskens, P. T.; Beurskens, G.; de Gelder, R.; Smits, J. M. M.; Garcia-Granda, S.; Gould, R. O. *DIRDIF2007*; Nijmvegen: The Netherlands, 2007.
(52) Nardelli, M. *J. Appl. Crystallogr.* **1982**, *6*, 6139.
(53) Nardelli, M. *J. Appl. Crystallogr.* **1999**, *32*, 563.
(54) Cramer, C. J. *Essentials of Computational Chemistry*, 2nd ed.; Wiley-VCH: New York, 2004; Chapter 9.1.3.

Table 3. Crystallographic Data

	$[Cu(L^3)(OH_2)]$-$(ClO_4)_2$ H_2O	$[Cu(L^{10})(NCCH_3)]$-$(BF_4)_2$ 1.4 $NCCH_3$	$[Cu(L^{11})(NCCH_3)]$-$(BF_4)_2$ $NCCH_3$ 0.5 H_2O	$[Cu(L^{12})(OH_2)]$-$(CF_3SO_3)_2$ H_2O
formula	$C_{25}H_{36}Cl_2CuN_4O_{16}$	$_{33.85}H_{38.26}B_2CuF_8N_{7.43}O_5$	$C_{34}H_{40}B_2CuF_8N_7O_{5.50}$	$C_{33}H_{41}CuF_6N_5O_{14}S_2$
cryst syst	triclinic	monoclinic	triclinic	monoclinic
space group	$P\bar{1}$	$C2/c$	$P\bar{1}$	$P2_1/c$
a/Å	11.3296(5)	24.298(2)	8.4311(10)	21.4370(12)
b/Å	11.8347(5)	8.5353(8)	12.8531(15)	11.1418(6)
c/Å	12.2378(6)	37.278(4)	18.681(2)	16.7592(9)
α/deg	105.410(1)		100.754(2)	
β/deg	98.250(1)	103.450(2)	92.115(2)	96.9510(10)
γ/deg	92.775(1)		107.401(2)	
V /Å^3	1559.1(1)	7519.1(12)	1888.5(4)	3973.5(4)
Z	2	8	2	4
M_r	783.02	866.29	871.89	973.37
d_c/Mg m^{-3}	1.668	1.531	1.533	1.627
F_{000}	810	3555	896	2004
μ(Mo Kα) /mm^{-1}	0.955	0.673	0.671	0.756
max., min. transmission factors	0.8705, 0.7826	0.7456, 0.6648	0.7463, 0.6366	0.9342, 0.8725
ϑ range/deg	1.8−32.0	1.7−25.0	1.7−28.7	1.0−28.7
index ranges (indep. set) h,k,l	−16 to +16, −17 to +17, 0 to +18	−28 to +28, 0 to +10, 0 to +44	−11 to +11, −17 to +17, 0 to +25	−28 to +28, 0 to +15, −22 to 0
reflns measured	28095	42276	28355	57415
unique, R_{int}	10598, 0.0281	6639, 0.0998	9764, 0.0649	10268, 0.0693
observed [$I \geq 2\sigma(I)$]	9263	4301	6962	7212
params refined	450	540	530	568
R indices [$F > 4\sigma(F)$] $R(F)$, $wR(F^2)$	0.0426, 0.1161	0.0772, 0.1945	0.0599, 0.1414	0.0421, 0.0979
R indices (all data) $R(F)$, $wR(F^2)$	0.0488, 0.1204	0.1336, 0.2294	0.0971, 0.1703	0.0683, 0.1071
GoF on F^2	1.108	1.366	1.034	1.054
largest residual peaks/e Å^{-3}	2.036, −1.165	2.031, −1.012	1.815, −1.198	0.499, −0.636

Molecular Operating Environment.[55] The parameters were developed with respect to the MMFF94 force field distributed with MOE (see Table S1, Supporting Information). LFMM parameters for pyridyl nitrogen (MMFF atom type NPYD), amine (atom type N), and imidazolyl nitrogen (atom type N5B) were adapted from previous studies,[26,32] and these, plus the remaining parameters, were further refined using the X-ray structures of systems with ligands L^1 through L^{12}. Alternative local minima corresponding to variations in the Jahn−Teller axis were searched for by manually setting all of the Cu−L distances to appropriate values, relaxing the rest of the molecule, and then fully optimizing the resulting structure. This process was tested for several systems via 1000-step stochastic searches where starting configurations are generated by adding random increments to the torsion angles of all rotatable bonds. The automated search process gave the same results.

Acknowledgment. Generous financial support by the German Science Foundation (DFG) is gratefully acknowledged. R.J.D. acknowledges the support of Chemical Computing Group and the EPSRC Chemical Database Service.

Supporting Information Available: CIF files giving crystallographic data for compounds $[Cu(L^3)(OH_2)](ClO_4)_2 \cdot H_2O$, $[Cu(L^{10})(NCCH_3)](BF_4)_2 \cdot 1.4$ $NCCH_3$, $[Cu(L^{11})(NCCH_3)](BF_4)_2 \cdot NCCH_3 \cdot 0.5$ H_2O, and $[Cu(L^{12})(OH_2)](CF_3SO_3)_2 \cdot H_2O$. This material is available free of charge via the Internet at http:/pubs.acs.org.

IC8011052

(55) *MOE Molecular Operation Environment*, 2007.09; Chemical Computing Group: Montreal, Canada, 2007.
(56) Börzel, H.; Comba, P.; Katsichtis, C.; Kiefer, W.; Lienke, A.; Nagel, V.; Pritzkow, H. *Chem.−Eur. J.* **1999**, *5*, 1716.